Hindawi Publishing Corporation
EURASIP Journal on Wireless Communications and Networking
Volume 2010, Article ID 678490, 12 pages
doi:10.1155/2010/678490

Research Article

Spatial Capacity of UWB Networks with Space-Time Focusing Transmission

Yafei Tian and Chenyang Yang

School of Electronics and Information Engineering, Beihang University, Beijing 100191, China

Correspondence should be addressed to Yafei Tian, ytian@buaa.edu.cn

Received 3 August 2010; Accepted 29 November 2010

Academic Editor: Claude Oestges

Space-time focusing transmission in impulse-radio ultra-wideband (IR-UWB) systems resorts to the large number of resolvable paths to reduce the interpulse interference as well as the multiuser interference and to simplify the receiver design. In this paper, we study the spatial capacity of IR-UWB systems with space-time focusing transmission where the users are randomly distributed. We will derive the power distribution of the aggregate interference and investigate the collision probability between the desired focusing peak signal and interference signals. The closed-form expressions of the upper and lower bound of the outage probability and the spatial capacity are obtained. Analysis results reveal the connections between the spatial capacity and various system parameters and channel conditions such as antenna number, frame length, path loss factor, and multipath delay spread, which provide design guidelines for IR-UWB networks.

1. Introduction

Impulse-radio ultra-wideband (IR-UWB) signals have large bandwidth, which can resolve a large number of multipath components in densely scattered channels. For communication links connecting different pairs of users, the correlation between multipath channel coefficient vectors is weak even when the user positions are very close [1, 2]. Exploiting these characteristics, time-reversal (TR) prefiltering technique was proposed in IR-UWB communications [3–5], which can focus the signal energy to a specific time instant and geometrical position.

The space-time focusing transmission has been widely studied in underwater acoustic communications [6, 7], and UWB radar and imaging areas [8–10]. In UWB communications, TR technique is usually used to provide low complexity receiver [3–5]. By prefiltering the signal at the transmitter side with a temporally reversed channel impulse response, the received signal will have a peak at the desired time and location. The physical channel behaves as a spatial-temporal matched filter. In time domain, the focused peak is a low duty-cycle signal; thus interpulse interference reduces and a simple one-tap receiver can be used. In space domain, the strong signal only appears at one spot, thus mutual interference among coexisting users can be mitigated. This is exploited for multiuser transmission in [11], where different users employ time-shifted channel impulse responses as their prefilters.

TR techniques were evolved to multiantenna transmission in recent years. Applying TR technique for multiple input single output (MISO) systems was investigated by experiments in [12–14], and for multiple input multiple output systems (MIMO) was studied in [2, 15, 16]. With multiple antennas, the focused area is sharper both in time and in space domains [17], thereby the interference is significantly mitigated. To achieve better interference suppressing capability than TR prefilter, advanced preprocessors based on zero-forcing and minimum-mean-square-error criteria were used in [18, 19]. To reduce the preprocessing complexity and the feedback overhead for acquiring the channel information, a precoder based on channel phase information was proposed in [20], where the performance loss is nevertheless unavoidable. A general precoding framework for UWB systems, where the codeword can take any real value, is considered in [21]. The detection performance is traded

off with the communication and computational cost by adjusting the number of bits to represent each codeword.

IR-UWB communications are favorable for *ad hoc* networks with randomly distributed nodes, where transmission links are built in a peer-to-peer manner. Although experiment results demonstrate that space-time focusing transmission leads to much lower sidelobes of the transmitted signal, the impact of such kind of interference on the accommodable user density and spatial capacity has not been studied, as far as the authors know. For a given outage probability, the spatial capacity is the maximal sum transmission rate of all users who can communicate peer-to-peer simultaneously in a fixed area.

In a landmark paper of *ad hoc* network capacity [22], the authors showed that the throughput for each node vanishes with $\sqrt{n}$, when the channel is shared by n identical randomly located nodes with random access scheme. Some results of user capacity for direct sequence code-division multi-access (DS-CDMA) and frequency hopping (FH)-CDMA systems were presented in [23, 24]. Essentially, space-time focusing transmission in IR-UWB systems accesses the channel with a combined random time-division and random code-division scheme. On one hand, IR-UWB signals are low duty-cycle. After the prefiltering and multipath propagation, the cochannel interference signals are low duty-cycle as well if the interpulse interference are absent. On the other hand, the cochannel interference has a random power and occupies partial time of the pulse repetition period. The performance of the desired user degrades only when its focused peak collides with interference signals and the aggregate interference power exceeds its desired tolerance. The random propagation delay of the low duty-cycle signal leads to a random accessing time, and the random multipath response of the communication link induces a random "spreading code". Large number of multipath components will provide high "spreading gain", but may also lead to large collision probability. The combined impact on the spatial capacity is still not well understood.

In this paper, we model the aggregate interference powers as two heavy-tailed distributions, that is, Cauchy and Lévy distributions, when path loss factor is 2 or 4. These yield explicit expressions of upper and lower bounds of the spatial capacity, which shows clearly the connections between the spatial capacity and the frame length, multipath delay spread, pulse width, transmit antenna number, link distance and outage probability constraint, and so forth. We also obtain optimal interference tolerance for each transmission link that maximizes the spatial capacity in different channel conditions.

The rest of this paper is organized as follows. Section 2 introduces the network setting and the UWB space-time focusing transmission system. Then in Sections 3 and 4 the outage probability in additive white Gaussian noise (AWGN) channels and in multipath and multiantenna channels are, respectively, derived. Section 5 presents the closed-form expressions of the accommodable user density and the spatial capacity. Simulation and numerical results are provided in Section 6 to verify the theoretical analysis. The paper is concluded in Section 7.

2. System Description

We consider *ad hoc* networks without coordinators, where half-duplex nodes are distributed uniformly within a circle, as shown in Figure 1(a). Each node is either a transmitter or a receiver. Without loss of generality, we regard the receiver at the center as the desired user and all transmitters except the desired one as the interference users. This is an interference channel problem, whose equivalent model is shown in Figure 1(b). The link distance of the desired transmitter and receiver is r_D, while the link distances between the interference transmitters and the desired receiver are random variables whose values are less than a threshold distance r_T, where $r_T \gg r_D$. The weak interference outside r_T are neglected. We will show in Section 5 that such a threshold distance is unnecessary when we consider the per area user capacity.

In IR-UWB systems, the transmitted signals are pulse trains modulated by the information data. For brevity, we only consider the pulse amplitude modulation, since the spreading gain and collision probability of the pulse position modulation will be the same with a random transmit delay.

In AWGN channels, the channel response $h(t) = \delta(t)$, then the TR prefilter is also $\delta(t)$. The transmitted signal of the kth user is

$$s^{(k)}(t) = \sum_i \sqrt{P_t T_s} x_i^{(k)} p(t - iT_s), \tag{1}$$

where P_t is the transmit power, $x_i^{(k)}$ is the ith data symbol, $p(t)$ is the UWB short pulse with width T_p and normalized energy, and T_s is the pulse repetition period or the frame length in UWB terminology. In each frame, there are $N_s = T_s/T_p$ time slots.

In multipath channels, define the channel response between the transmitter j and the receiver k as

$$h_{j,k}(t) = \sum_{l=1}^{L(j,k)} a_l(j,k)\delta(t - \tau_l(j,k)), \tag{2}$$

where $L(j,k)$ is the total number of specular reflection paths with amplitude $a_l(j,k)$ and delay $\tau_l(j,k)$.

Since the channel response does not have imaginary part in IR-UWB systems, the TR prefilter at the kth transmitter for the kth receiver is $h_{k,k}(-t)$, and the transmitted signal is

$$\tilde{s}^{(k)}(t) = s^{(k)}(t) * h_{k,k}(-t), \tag{3}$$

where "$*$" denotes convolution operation.

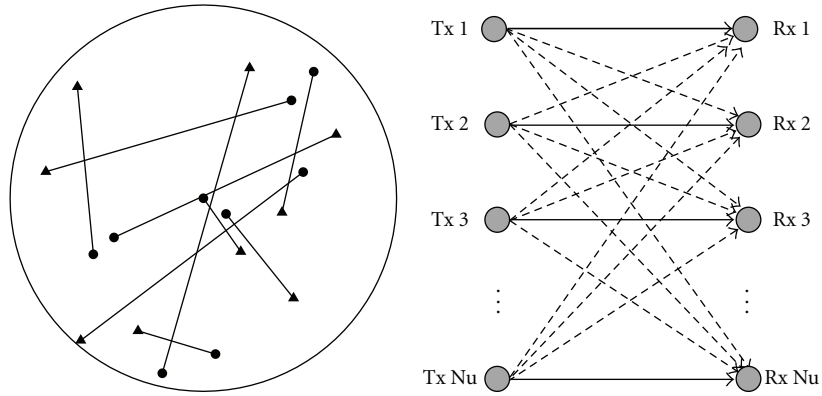

Figure 1: (a) Randomly distributed nodes in *ad hoc* networks, where the solid triangles denote transmitters and the solid circles denote receivers. (b) Interference channel model.

At the intended receiver k, the received signal is a summation of the signals from all N_u coexisting users that are further filtered by the multipath channels, that is,

$$\begin{aligned} r^{(k)}(t) &= \sum_{j=0}^{N_u-1} A_{j,k}\tilde{s}^{(j)}\left(t-\tau_{j,k}\right) * h_{j,k}(t) + z(t) \\ &= A_{k,k}s^{(k)}(t-\tau_{k,k}) * h_{k,k}(-t) * h_{k,k}(t) \\ &\quad + \underbrace{\sum_{j=0, j\neq k}^{N_u-1} A_{j,k}s^{(j)}(t-\tau_{j,k}) * h_{j,j}(-t) * h_{j,k}(t)}_{\text{Cochannel Interference}} \\ &\quad + z(t), \end{aligned} \tag{4}$$

where $A_{j,k}$ and $\tau_{j,k}$ are the signal amplitude attenuation and random propagation delay from the transmitter j to the receiver k, respectively, and $z(t)$ is the AWGN.

Since the prefilter $h_{k,k}(-t)$ matches with the channel response $h_{k,k}(t)$, there will be a focused peak at $t = iT_s + \tau_{k,k}$, that involves the desired information from transmitter k. The unintended cochannel interference from other transmitters behaves as random dispersions since $h_{j,j}(t)$ and $h_{j,k}(t)$ are weakly correlated.

When each transmitter equips with M antennas, the channel responses from each transmit antenna to the receive antenna are different. As a result, the prefilters at different transmit antennas are different. Denote the channel response and the propagation delay from the mth antenna of the transmitter j to the receiver k as $h_{j,k,m}(t)$ and $\tau_{j,k,m}$, and the average propagation delay from the transmitter j to the receiver k as $\tau_{j,k}$, respectively. Define $\Delta_{j,k,m} = \tau_{j,k,m} - \tau_{j,k}$ as the transmit delay at the mth antenna; then the transmitted signal at the mth antenna of transmitter k is

$$\tilde{s}_m^{(k)}(t) = s^{(k)}(t+\Delta_{k,k,m}) * h_{k,k,m}(-t), \tag{5}$$

and the received signal of the desired user is

$$r^{(k)}(t) = \sum_{j=0}^{N_u-1} A_{j,k} \sum_{m=0}^{M-1} \tilde{s}_m^{(j)}\left(t-\tau_{j,k,m}\right) * h_{j,k,m}(t) + z(t), \tag{6}$$

where the amplitude attenuation coefficient $A_{j,k}$ reflects the large-scale fading between the transmitter j and the receiver k, $h_{j,k,m}(t)$ is the small-scale fading. From each antenna of transmitter k, there is a focused signal; these M peaks will all arrive at time instant $t = iT_s+\tau_{k,k}$ and accumulate coherently, thus an array gain M can be obtained.

Assume that there is no intersymbol interference. The receiver k can apply a pulse-matched filter and then simply sample the focused peak for detection. The sampled signal is

$$r^{(k)}[i] = r^{(k)}(t) * p(-t)\Big|_{t=iT_s+\tau_{k,k}}. \tag{7}$$

In these samples, the signal energy from the desired transmitter k is fully collected, while only parts of the energy from interferers are present due to the dispersion of interference signals. This leads to a power gain which is referred to as *spreading gain* because of its similarity with the gain obtained in conventional spreading systems. The value of this gain depends on the delay spread and cross-correlation of channel responses $h_{j,j,m}(t)$ and $h_{j,k,m}(t)$.

When the duration of $h_{j,j,m}(-t) * h_{j,k,m}(t)$ is less than the frame length T_s, the signal from transmitter j may not collide with the focused peak, thereby does not degrade the detection performance of the desired user k. Long T_s will produce low collision probability. This leads to another gain to mitigate the interference which is referred to as *time-focusing gain*. The value of this gain approximately depends on the ratio of the frame length and the multipath delay spread, as will be shown in Section 4.

When multiple antennas are used in each transmitter, the array gain obtained is in fact a *space-focusing gain*. Since the focused signals from M antennas arrive at the same time, the number of transmit antennas does not affect the collision probability between the desired signal and the interference.

The value of this gain depends only on the antenna number, that is, $G_A = M$.

3. Outage Probability in AWGN Channels

Outage probability is an important measure for transmission reliability. In the considered system, the outage probability depends on the number of interference users. When the interference from other users collides with the focused peak signal and the aggregate interference power exceeds the tolerance of the intended receiver, an outage happens. The spatial capacity is obtained as the maximal accommodable user number multiplied by the single-user transmission rate given the outage probability constraint.

In this section, we will derive the outage probability of IR-UWB systems in AWGN channels. We will first study the distribution of single-user interference and aggregate interference; then the collision probability between the desired and interference pulse signals is derived. The outage probability is finally obtained considering both the impact of interference power and the impact of collision probability. The benefit of using interference avoidance techniques will also be addressed.

It should be noted that we consider different path loss factors here, which may be an abuse of the concept of "AWGN channel". Despite that AWGN channel is appropriate for modeling free-space propagation environment where path loss factor is 2, the results in this section facilitate the derivation of the outage probability in multipath and multiple antenna channels later. In AWGN channels, each pulse is assumed to occupy one time slot, thus the pulses of different users may collide completely or do not collide at all.

3.1. The Statistics of Single-User Interference. In AWGN channels, the received signals are the combined pulse trains from all users with different delays. When the pulses from different users fall in the same time slot, mutual interference will appear. Consider one interference user whose distance to the desired user is r. Since the interference users are uniformly distributed inside a circle with the radius r_T, the PDF of r is

$$f_r(x) = \frac{2x}{r_T^2}, \quad x \le r_T. \tag{8}$$

The interference power depends on the propagation distance r and the path loss factor α, that is, [25]

$$P_r = P_t\left(\frac{4\pi f_c r_0}{v_c}\right)^{-2}\left(\frac{r}{r_0}\right)^{-\alpha} = P_0 r^{-\alpha}, \tag{9}$$

where $P_0 = P_t v_c^2 r_0^\alpha/(4\pi f_c r_0)^2$ is the received power at a reference distance r_0, f_c is the center frequency, and v_c is the light speed. Note that the expression (9) is only exact in narrow-band systems, since in UWB systems P_0 cannot be determined only by the center frequency. Nonetheless, in the following analysis we will normalize the received power by P_0, thereby this will not affect the derived outage probability. In free space propagation, the path loss factor $\alpha = 2$, while in urban propagation environments, the path loss factor can be as large as 4. Other values of α between 2 and 4 reflect various propagation environments in suburban and rural areas.

Knowing the PDF of the interference distance as shown in (8), we can then obtain the PDF of the interference power as

$$\begin{aligned} f_{P_r}(x) &= \frac{2P_0^{2/\alpha}}{\alpha r_T^2}x^{-(2/\alpha)-1}, \quad x \ge P_0 r_T^{-\alpha}, \\ &= \begin{cases} \dfrac{P_0}{r_T^2}x^{-2}, & \alpha = 2, \\ \dfrac{2P_0^{2/3}}{3r_T^2}x^{-5/3}, & \alpha = 3, \\ \dfrac{\sqrt{P_0}}{2r_T^2}x^{-3/2}, & \alpha = 4. \end{cases} \end{aligned} \tag{10}$$

It shows that P_r has a heavy-tailed distribution, which means that its tail probability decays with the power law instead of the exponential law [26].

To simplify the notations, we define a normalized interference power as

$$\lambda = \frac{P_r}{P_0 r_T^{-\alpha}}. \tag{11}$$

Its PDF can be obtained as

$$\begin{aligned} f_\lambda(x) &= \frac{2}{\alpha}x^{-(2/\alpha)-1}, \quad x \ge 1, \\ &= \begin{cases} \dfrac{1}{x^2}, & \alpha = 2, \\ \dfrac{2}{3x^{5/3}}, & \alpha = 3, \\ \dfrac{1}{2x^{3/2}}, & \alpha = 4. \end{cases} \end{aligned} \tag{12}$$

3.2. The Statistics of Aggregate Interference. When there are more than one interference users, the PDF of the aggregate interference power is the multifold convolutions of (12). It is hard to obtain its closed-form expression. Observing (12), we find that the distribution of λ can be approximated by Cauchy distribution when $\alpha = 2$, and by Lévy distribution when $\alpha = 4$. Cauchy distribution and Lévy distribution are both heavy-tailed stable distributions and their PDFs have explicit expressions (Stable distributions generally do not have explicit expressions of their density functions, except three special cases, i.e., Gaussian, Cauchy, and Lévy distributions.) A random variable is stable when a linear combination of two independent copies of the variable has the same distribution, except that the location and scale parameters vary [26]. Therefore, if we model the interference power from one user as Cauchy or Lévy distribution, the aggregate interference power from multiple users will also has a Cauchy or Lévy distribution. This allows us to obtain closed-form expressions of the outage probabilities. Furthermore, we can use the PDFs of Cauchy and Lévy distributions as the lower and upper bounds of (12) to

accommodate various values of α, that is, to investigate the impact of various propagation environments.

Cauchy distribution has a PDF as [26]

$$f(x;x_0,b)=\frac{1}{\pi}\left[\frac{b}{(x-x_0)^2+b^2}\right],\quad -\infty<x<\infty \tag{13}$$

and has a cumulative distribution function (CDF) as [26]

$$F(x;x_0,b)=\frac{2}{\pi}\arctan\left(\frac{x-x_0}{b}\right), \tag{14}$$

where x_0 is the location parameter indicating the peak position of the PDF, and b is the scale parameter indicating when the PDF decays to one half of its peak value. When n independent random variables of Cauchy distribution with the same location and scale parameters add together, their sum still follows Cauchy distribution where the location parameter becomes nx_0 and the scale parameter becomes nb.

When $\alpha=2$, the PDF of λ can be lower bounded by a Cauchy distribution with $x_0=0$ and $b=\pi/2$, that is,

$$f_\lambda\left(x;0,\frac{\pi}{2}\right)=\frac{1}{x^2+\pi^2/4}, \tag{15}$$

where the coefficient $1/\pi$ in standard Cauchy distribution is replaced by $2/\pi$ because of the single-sided constraint $\lambda\geq 1$, so that the integral of $f_\lambda(x)$ over λ is still 1.

The sum of n independent copies of λ, defined as Λ_n, still follows Cauchy distribution without considering the constraint $\lambda\geq 1$. The CDF of Λ_n can be obtained as

$$F_{\Lambda_n}\left(x;0,\frac{\pi}{2}\right)=\frac{2}{\pi}\arctan\left(\frac{2x}{n\pi}\right). \tag{16}$$

When the constraint is considered, the practical PDF of Λ_n has heavier tail than that obtained by Cauchy distribution, and thus the practical CDF of Λ_n is smaller than $F_{\Lambda_n}(x;0,\pi/2)$. However, we will see in the later simulations that (16) is a quite tight bound when few interference users exist.

Lévy distribution has a PDF as [26]

$$f(x;x_0,c)=\sqrt{\frac{c}{2\pi}}\frac{e^{-c/2(x-x_0)}}{(x-x_0)^{3/2}},\quad x_0\leq x<\infty \tag{17}$$

and has a CDF as [26]

$$F(x;x_0,c)=\operatorname{erfc}\left(\sqrt{\frac{c}{2(x-x_0)}}\right), \tag{18}$$

where x_0 is the location parameter, c is the scale parameter, and $\operatorname{erfc}(\cdot)$ is the complementary error function, which is defined as $\operatorname{erfc}(x)=(2/\sqrt{\pi})\int_x^\infty e^{-t^2}dt$. Both $f(x;x_0,c)$ and $F(x;x_0,c)$ are equal to 0 if $x<x_0$. When n independent random variables of Lévy distribution with the same location and scale parameters add together, their sum still follows Lévy distribution where the location parameter becomes nx_0 and the scale parameter turns to be n^2c.

When $\alpha=4$, the PDF of λ can be approximated by a Lévy distribution with $x_0=1$ and $c=\pi/2$, that is,

$$f_\lambda\left(x;1,\frac{\pi}{2}\right)=\frac{1}{2}\left[\frac{e^{-\pi/4(x-1)}}{(x-1)^{3/2}}\right], \tag{19}$$

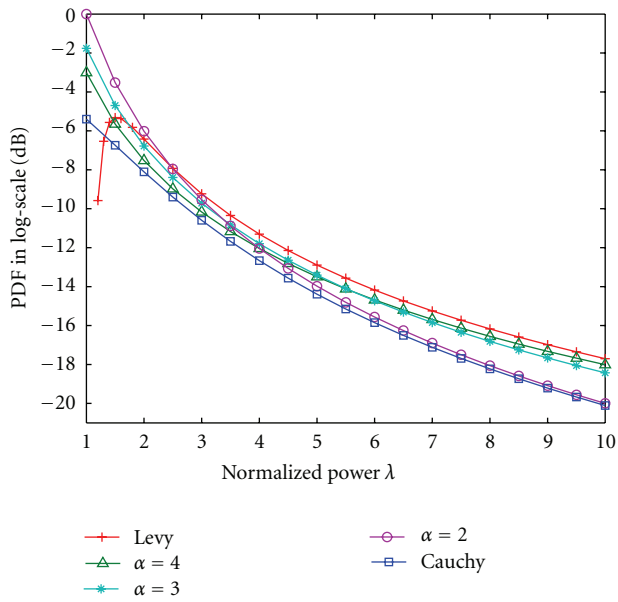

Figure 2: The PDFs of Cauchy and Lévy distribution, as well as the practical PDFs of the normalized interference power λ when $\alpha=2$, 3, and 4.

where the constraint $\lambda\geq 1$ is satisfied by the definition of Lévy distribution.

Using this bound, the CDF of the sum interference power Λ_n can be obtained as

$$F_{\Lambda_n}\left(x;1,\frac{\pi}{2}\right)=\operatorname{erfc}\left(\sqrt{\frac{n^2\pi}{4(x-n)}}\right). \tag{20}$$

Figure 2 shows the practical PDFs of the normalized interference power λ when $\alpha=2,3,4$, as well as the lower and upper bound obtained by Cauchy and Lévy distribution, respectively. We can see that the bounds are tight when the interference powers are strong.

3.3. Outage Probability. Similar to (11), we define the normalized signal power as

$$\lambda_D=\frac{P_0r_D^{-\alpha}}{P_0r_T^{-\alpha}}=\frac{r_T^\alpha}{r_D^\alpha}. \tag{21}$$

Assume that the required signal-to-interference-plus-noise-ratio (SINR) for reliable transmission is

$$\beta=\frac{\lambda_D}{\lambda_N+\lambda_I}, \tag{22}$$

where $\lambda_N = P_N/(P_0 r_T^{-\alpha})$ is the normalized noise power. If the SNR of the desired user is given as γ, that is, $\lambda_D/\lambda_N = \gamma$, then the normalized interference power tolerance will be

$$\lambda_I = \left(\frac{1}{\beta} - \frac{1}{\gamma}\right)\lambda_D = \mu \frac{r_T^\alpha}{r_D^\alpha}, \tag{23}$$

where $\mu = 1/\beta - 1/\gamma$. The communication will break when the normalized interference power exceeds λ_I.

We first consider that the pulses from n interference users arrive at the same time slot with that of the desired user, then the outage probability of the desired user is

$$\begin{aligned} P(\Lambda_n > \lambda_I) &= 1 - F_{\Lambda_n}(\lambda_I) \\ &= \begin{cases} \operatorname{erf}\left(\sqrt{\dfrac{n^2\pi}{4(\lambda_I - n)}}\right), & \text{UB}, \\ \dfrac{2}{\pi}\arctan\left(\dfrac{n\pi}{2\lambda_I}\right), & \text{LB}, \end{cases} \end{aligned} \tag{24}$$

where $\operatorname{erf}(x) = 1 - \operatorname{erfc}(x)$ is the error function, "UB" stands for upper bound, and "LB" stands for lower bound. The upper bound is derived from Lévy distribution and the lower bound is from Cauchy distribution.

Since there are N_s time slots in a frame, if there are N_u interference users in total, then the number of users that occupy the same time slot with the desired user is a random variable. The probability that n users collide with the desired user is

$$\begin{aligned} p_{N_u}(n) &= C_{N_u}^n \left(\frac{1}{N_s}\right)^n \left(\frac{N_s - 1}{N_s}\right)^{N_u - n} \\ &= \frac{C_{N_u}^n (N_s - 1)^{N_u - n}}{N_s^{N_u}}, \quad n = 1, \ldots, N_u, \end{aligned} \tag{25}$$

where $C_{N_u}^n$ is the binomial coefficient for n out of N_u. It is apparent that increasing N_s will reduce the collision probability and thus reduce the average outage probability. This is the benefit brought by the low duty-cycle characteristic of the IR-UWB signals.

The average outage probability is the summation of all the possibilities that n users generate interference and their aggregate power exceeds the designed tolerance, that is,

$$\begin{aligned} &P_{\text{out}}(N_u) \\ &= \sum_{n=1}^{N_u} p_{N_u}(n) P(\Lambda_n > \lambda_I) \\ &= \begin{cases} \displaystyle\sum_{n=1}^{N_u} \frac{C_{N_u}^n (N_s - 1)^{N_u - n}}{N_s^{N_u}} \left[\operatorname{erf}\left(\sqrt{\frac{n^2\pi}{4(\lambda_I - n)}}\right)\right], & \text{UB}, \\ \displaystyle\sum_{n=1}^{N_u} \frac{C_{N_u}^n (N_s - 1)^{N_u - n}}{N_s^{N_u}} \left[\frac{2}{\pi}\arctan\left(\frac{n\pi}{2\lambda_I}\right)\right], & \text{LB}. \end{cases} \end{aligned} \tag{26}$$

Remarks 1. If the desired user can avoid the interference by transmitting at a slot with minimal interference power, then the outage only happens when no time slot is available for transmission, that is, the interference power is larger than the designed tolerance λ_I in all the N_s time slots. As a result, the outage probability is reduced to

$$\widetilde{P}_{\text{out}}(N_u) = [P_{\text{out}}(N_u)]^{N_s}. \tag{27}$$

This is the minimum outage probability that an uncoordinated IR-UWB network is able to achieve.

If all the users can further coordinate their transmit delays, the interference signals from all links may be aligned to occupy only part of the frame period excluding the slot used by the desired user, then interference-free transmission can be realized. The transmission scheme design for interference alignment is out of the scope of this paper, which can be found from [27, 28] and the references therein.

4. Outage Probability in Multipath and Multiantenna Channels

In multipath channels with TR transmission, large multipath delay spread provides high spreading gain but induces high collision probability among users. In this section, we will first derive the spreading gain and collision probability, respectively, given the power delay profile of the multipath channels. Then the expressions of the outage probability in multipath channels with and without multiantennas in each transmitter will be developed.

4.1. Spreading Gain and Collision Probability. It is known that the small-scale fading of UWB channels is not severe. Therefore, it is reasonable to assume that the received signal power only depends on the path loss and the shadowing [1, 29]. Assume that $\int_0^\infty |h_{i,j}(t)|^2 dt = 1$, that is, the energy of multipath channel is normalized, and $\tau_{\max} < T_s$, that is, there is no ISI.

Assume that the channel's power delay profile subjects to exponential decay (For mathematical tractability; here we employ a simple UWB channel model without considering the cluster features. The more realistic IEEE 802.15.4a channel model will be used in simulations to verify the analytical results), that is,

$$D(\tau) = \frac{1}{\tau_{\text{RMS}}} e^{-\tau/\tau_{\text{RMS}}}, \quad \tau > 0, \quad \int_0^\infty D(\tau) d\tau = 1, \tag{28}$$

where τ_{RMS} is the root-mean-square (RMS) delay spread of the channel.

From (4), we know that the composite response, that is, the convolution of the prefilter and the channel, of the desired channel is $\widetilde{h}_{k,k}(t) = h_{k,k}(-t) * h_{k,k}(t)$, which has a focusing peak at $t = 0$ and the energy of the peak is $\int_0^\infty |h_{k,k}(t)|^2 dt = 1$. The duration of the peak signal is $2T_p$ due to the pulse-matched filter, thus its power is $1/2T_p$.

Similarly, the composite response of the interference channel is $\widetilde{h}_{j,k}(t) = h_{j,j}(-t) * h_{j,k}(t)$, which is a random process and the average power is obtained as

$$\begin{aligned} E\left[\left|\widetilde{h}_{j,k}(t)\right|^2\right] &= \int_0^\infty E\left[\left|h_{j,j}(\tau - t)\right|^2\right] E\left[\left|h_{j,k}(\tau)\right|^2\right] d\tau \\ &= \int_0^\infty D(\tau - t) D(\tau) d\tau \\ &= \frac{1}{2\tau_{\mathrm{RMS}}} e^{-|t|/\tau_{\mathrm{RMS}}}, \end{aligned} \tag{29}$$

where the first equality comes from the uncorrelated property of the two channels.

We can see that the average interference channel power subjects to double-sided exponential decay. To obtain explicit expressions of the spreading gain and the collision probability, we approximate the profile of the average interference power by a rectangle with the same area. The impact of this approximation will be shown through simulations in Section 6.

Since the sum power of the interference channel is

$$\int_{-\infty}^{\infty} \frac{1}{2\tau_{\mathrm{RMS}}} e^{-|t|/\tau_{\mathrm{RMS}}} dt = 1, \tag{30}$$

and the maximal value of (29) is $1/2\tau_{\mathrm{RMS}}$, the rectangle has a length $2\tau_{\mathrm{RMS}}$ given the height $1/2\tau_{\mathrm{RMS}}$. Then the approximated interference channel power will always be $1/2\tau_{\mathrm{RMS}}$ in a duration of $2\tau_{\mathrm{RMS}}$.

Since the desired channel has a power $1/2T_p$ and the interference channel has a power $1/2\tau_{\mathrm{RMS}}$, the spreading gain can be obtained as

$$G_S = \frac{1/2T_p}{1/2\tau_{\mathrm{RMS}}} = \frac{\tau_{\mathrm{RMS}}}{T_p}, \tag{31}$$

which reflects the interference suppression capability of the TR prefilter in multipath channels.

Since the frame length is T_s and the approximated interference duration is $2\tau_{\mathrm{RMS}}$, the probability that the signal of one interference user collides with the focused peak of the desired user is approximately

$$\delta = \frac{2\tau_{\mathrm{RMS}}}{T_s} = \frac{2G_S}{N_s}. \tag{32}$$

The reciprocal of δ is actually the time-focusing gain, that is,

$$G_T = \frac{T_s}{2\tau_{\mathrm{RMS}}} = \frac{N_s}{2G_S}, \tag{33}$$

which reflects the interference mitigation capability of TR prefilter through near orthogonal sharing of the time resource by exploiting the low duty cycle feature of IR-UWB signals.

When totally N_u users exist, the probability that n users simultaneously interfere with the desired user is

$$p_{N_u}(n) = C_{N_u}^n \delta^n (1 - \delta)^{N_u - n}. \tag{34}$$

4.2. Outage Probability. Due to the spreading gain, the influence of interference on the decision statistics in multipath channels reduces to $1/G_S$ of that in AWGN channels when the same interference power is received. Consequently, when there are n interference signals, an outage happens when the sum power of the interference signals Λ_n exceeds $G_S\lambda_I$. Then the average outage probability in multipath channels is

$$P_{\mathrm{out}}(N_u) = \sum_{n=1}^{N_u - 1} p_{N_u}(n) P(\Lambda_n > G_S\lambda_I). \tag{35}$$

When each transmitter equips with M antennas, the output power at each antenna reduces to $1/M$ of that in single-antenna case. At the receiver, the desired signal will be increased by the array gain while both the interference power and the collision probability between the interference and the desired signals will not change.

Considering the antenna gain G_A, the spreading gain G_S, and the collision probability in multipath channel $p_{N_u}(n)$, the average outage probability when using multiple antennas is obtained as

$$\begin{aligned} P_{\mathrm{out}}(N_u) &= \sum_{n=1}^{N_u - 1} p_{N_u}(n) P(\Lambda_n > G_A G_S \lambda_I) \\ &= \begin{cases} \displaystyle\sum_{n=1}^{N_u} C_{N_u}^n \delta^n (1 - \delta)^{N_u - n} \\ \quad \times \left[\mathrm{erf}\left(\sqrt{\dfrac{n^2\pi}{4(G_A G_S \lambda_I - n)}} \right) \right], & \text{UB}, \\ \displaystyle\sum_{n=1}^{N_u} C_{N_u}^n \delta^n (1 - \delta)^{N_u - n} \\ \quad \times \left[\dfrac{2}{\pi} \arctan\left(\dfrac{n\pi}{2G_A G_S \lambda_I} \right) \right], & \text{LB}. \end{cases} \end{aligned} \tag{36}$$

This outage probability can also be reduced significantly if the desired user can choose a time slot with the lowest interference power for transmission, whose expression is identical to (27).

5. Spatial Capacity

5.1. Accommodable User Density. Given a required outage probability ϵ, the accommodable user number in the network can be expressed as

$$U = \max\{N_u \mid P_{\mathrm{out}}(N_u) \le \epsilon\}. \tag{37}$$

Observing (36), we find that the outage probability is associated with two terms, that is, $p_{N_u}(n)$ and $P(\Lambda_n > G_A G_S \lambda_I)$. The second term includes, respectively, an error function and an arctangent function in the upper and lower bounds. We can obtain much simpler expressions of these two functions by introducing approximations.

The Maclaurin series expansions of $\operatorname{erf}(x)$ and $\arctan(x)$ are

$$\begin{aligned}\operatorname{erf}(x) &= \frac{2}{\sqrt{\pi}}\sum_{n=0}^{\infty}\frac{(-1)^n x^{2n+1}}{n!(2n+1)} \\ &= \frac{2}{\sqrt{\pi}}\left(x-\frac{1}{3}x^3+\frac{1}{10}x^5-\frac{1}{42}x^7+\cdots\right), \\ \arctan(x) &= \sum_{n=0}^{\infty}\frac{(-1)^n x^{2n+1}}{2n+1} \\ &= x-\frac{1}{3}x^3+\frac{1}{5}x^5-\frac{1}{7}x^7+\cdots.\end{aligned} \tag{38}$$

When the outage probability is small, both the error function and the arctangent function can be approximated as linear functions, that is,

$$\operatorname{erf}(x) \approx \frac{2}{\sqrt{\pi}}x, \qquad \arctan(x) \approx x. \tag{39}$$

Using these approximations, (36) can be simplified as

$$P_{\text{out}}(N_u) = \begin{cases} \displaystyle\sum_{n=1}^{N_u} C_{N_u}^n \delta^n (1-\delta)^{N_u-n} \frac{n}{\sqrt{G_A G_S \lambda_I - n}}, & \text{UB}, \\ \displaystyle\sum_{n=1}^{N_u} C_{N_u}^n \delta^n (1-\delta)^{N_u-n} \frac{n}{G_A G_S \lambda_I}, & \text{LB}. \end{cases} \tag{40}$$

Remember from (23) that $\lambda_I = \mu r_T^\alpha / r_D^\alpha$; it will be much larger than n when the threshold distance r_T approaches infinity. Therefore, in the following approximations, we will replace the term $\sqrt{G_A G_S \lambda_I - n}$ with $\sqrt{G_A G_S \lambda_I}$ in the expression of upper bound.

Using the property

$$\begin{aligned}\sum_{n=1}^{N_u} C_{N_u}^n \delta^n (1-\delta)^{N_u-n} \frac{n}{\delta} &= N_u \sum_{n=1}^{N_u} C_{N_u-1}^{n-1} \delta^{n-1} (1-\delta)^{N_u-n} \\ &= N_u,\end{aligned} \tag{41}$$

and the relationship

$$G_S = \frac{\tau_{\text{RMS}}}{T_p} = \frac{\tau_{\text{RMS}}}{T_s/N_s} = \frac{N_s}{2G_T}, \tag{42}$$

the upper and lower bounds of the outage probability become

$$P_{\text{out}}(N_u) = \begin{cases} \dfrac{N_u}{G_T\sqrt{G_A G_S \lambda_I}} = \dfrac{2N_u\sqrt{\tau_{\text{RMS}} T_p}}{\sqrt{M\lambda_I} T_s}, & \text{UB}, \\ \dfrac{N_u}{G_T G_A G_S \lambda_I} = \dfrac{2N_u T_p}{M\lambda_I T_s}, & \text{LB}. \end{cases} \tag{43}$$

Therefore, given the outage probability constraint $P_{\text{out}}(N_u) = \epsilon$, the accommodable user number can be expressed as

$$U = \begin{cases} \epsilon G_T G_A G_S \lambda_I = \dfrac{\epsilon M \lambda_I T_s}{2T_p}, & \text{UB}, \\ \epsilon G_T \sqrt{G_A G_S \lambda_I} = \dfrac{\epsilon\sqrt{M\lambda_I} T_s}{2\sqrt{\tau_{\text{RMS}} T_p}}, & \text{LB}. \end{cases} \tag{44}$$

By contrast to the outage probability, the upper bound of the accommodable user number is obtained from Cauchy distribution which can be achieved when $\alpha = 2$ and the lower bound is obtained from Lévy distribution which can be achieved when $\alpha = 4$.

It is shown from (44) that increasing the time-focusing gain, the space-focusing gain and the spreading gain all lead to high accommodable user number. However, the increasing speed is different in terms of the upper bound and the lower bound. In fact, these three gains are not totally independent. The space-focusing gain can be provided by using more than one transmit antennas, but the spreading gain and the time-focusing gain both rely on the multipath channel response. As shown in (31) and (33), large delay spread will introduce high spreading gain but low time-focusing gain. As a result, it can be observed from (44) that longer channel delay spread will not lead to more coexisting users.

Upon substituting (23) into (44), we obtain the accommodable user density, that is, per area user number, as

$$\rho = \frac{U}{\pi r_T^2} = \begin{cases} \dfrac{\epsilon\mu M T_s}{2\pi r_D^2 T_p}, & \text{UB}, \\ \dfrac{\epsilon\sqrt{\mu M} T_s}{2\pi r_D^2 \sqrt{\tau_{\text{RMS}} T_p}}, & \text{LB}. \end{cases} \tag{45}$$

Then the auxiliary variable r_T vanishes, which is assumed in the beginning as an interference distance threshold.

5.2. Spatial Capacity. The expressions (44) and (45) tell us how many users can be accommodated in a given area. However, it does not fix the transmission rate of each user, thus the sum rate of all users; in a given area is not known.

In IR-UWB systems, the symbol rate R_s is determined by the reciprocal of the frame duration T_s, and the number of bits modulated on each symbol is determined by the SINR of the received signals. According to Shannon's channel capacity formula, the achievable transmission rate of each user will be

$$R_b = \frac{1}{T_s}\log_2(1+\beta), \tag{46}$$

given the SINR of the desired user β as in (22).

From (23) we know that, in interference-limited environment, the impact of cochannel interference is dominant and the impact of noise can be neglected; therefore, β can be

approximated as $1/\mu$. The sum data rate of all users in a unit area can be obtained as

$$R_{\text{sum}} = \rho R_b = \begin{cases} \dfrac{\epsilon\mu M}{2\pi r_D^2 T_p}\log_2\left(1+\dfrac{1}{\mu}\right), & \text{UB}, \\ \dfrac{\epsilon\sqrt{\mu M}}{2\pi r_D^2\sqrt{\tau_{\text{RMS}}T_p}}\log_2\left(1+\dfrac{1}{\mu}\right), & \text{LB}. \end{cases} \tag{47}$$

In the expression of the upper bound, the term $\mu\log_2(1+1/\mu)$ is a convex function of μ and it has a maximum value 1.44 when μ approaches infinity. In the expression of the lower bound, the term $\sqrt{\mu}\log_2(1+1/\mu)$ is also a convex function of μ. We can obtain its peak value by optimization algorithms, which is 1.16 when μ equals to 0.255. Substituting these results to (47), we obtain the maximal value of the sum rate, that is, the spatial capacity, as

$$S = \begin{cases} 0.72\dfrac{\epsilon M}{\pi r_D^2 T_p}, & \text{UB}, \\ 0.58\dfrac{\epsilon\sqrt{M}}{\pi r_D^2\sqrt{\tau_{\text{RMS}}T_p}}, & \text{LB}. \end{cases} \tag{48}$$

Through this expression, we can observe the impact of various parameters. In the following, we will analyze this expression and provide some insights into the design of the space-time focusing transmission UWB system.

5.3. Design Guidelines

5.3.1. Impact of Single-User Transmission Rate. It was seen from (48) that the spatial capacity is independent from two parameters μ and T_s. However, μ and T_s determine the single-user transmission rate as shown in (46), (22), and (23).

The spatial capacity depends on the single-user transmission rate through two ways. If the single-user transmission rate is enhanced by reducing T_s, the accommodable user number will be correspondingly decreased, and the spatial capacity will not be changed. This is why the spatial capacity does not depend on T_s.

There are optimal values of μ to maximize the upper and lower bounds of the sum data rate. For $\alpha = 2$, the optimal μ is infinity, that means the optimal SINR is infinitesimal. To ensure the error-free communications, it would be better to apply low-rate coding, low-level modulation, and large gain spreading, and so forth. For $\alpha = 4$, the optimal operating point is SINR = 6 dB ($1/\mu = 4$), which is a normal value for nonspreading communication system [30].

5.3.2. Impact of Path Loss Factor. When path loss factor is different, the relationship of the spatial capacity and the parameters M, τ_{RMS}, and T_p will differ. Since $\sqrt{\tau_{\text{RMS}}T_p} = \sqrt{G_S}T_p$, the upper bound is $1.24\sqrt{MG_S}$ larger than the lower bound. This indicates that large path loss factor will reduce the spatial capacity. When path loss factor is large, despite that both the desired signal power and the interference power attenuate faster, the aggregate inference power is more likely to exceed the interference tolerance given the total user number.

5.3.3. Impact of the Delay Spread. It can be observed that the delay spread does not affect the spatial capacity when $\alpha = 2$, whereas the spatial capacity decreases with $\sqrt{\tau_{\text{RMS}}}$ when $\alpha = 4$. As we have analyzed earlier, large delay spread will introduce high spreading gain, while it will also increase the collision probability among users. It can be seen from (44), when $\alpha = 2$, that there exists a balance between these two competing factors. However, when $\alpha = 4$, the effect of spreading gain is in square root, thus it cannot compromise the performance degradation led by the collisions.

5.3.4. Impact of the Array Gain. We can see that the spatial capacity grows linearly with the antenna number M when $\alpha = 2$ and grows sublinearly with $\sqrt{M}$ when $\alpha = 4$.

5.3.5. Impact of the Link Distance. It is shown that the spatial capacity decreases with r_D^2 no matter if the path loss factor equals to 2 or 4. As shown in (45), to guarantee a given outage probability, the user density will reduce when the coverage of the single-hop link increases.

5.3.6. Remarks. We have seen that the spreading gain and the time-focusing gain are mutually inhibited in improving the spatial capacity. To break such a balance, there are two possible approaches. The first one is to apply the interference avoidance technique, which makes the user access the channel at a time slot with weaker interference. The collision probability will therefore be reduced without altering the spreading gain. In a decentralized network, the interference avoidance might be hard to implement, since the optimal transmit time slot of one user depends on the transmit time slot of other users, and it will be soon changed if a user enters or leaves the network. Therefore, the decentralized interference coordinating schemes, such as the interference alignment technique [31, 32], would be studied to use in the space-time focusing UWB transmission systems in further researches.

The second approach is to apply advanced prefilters instead of TR prefilter, such as those introduced in [18, 19]. With an enhanced interference mitigation capability, a larger spreading gain can be obtained given the multipath channel delay spread, that is, the time-focusing gain.

6. Simulation and Numerical Results

In this section, we will verify the outage probability expressions derived in AWGN and multipath channels through simulations. Since the spatial capacity is obtained from these outage probability expressions, it can be verified also though indirectly.

In the simulations, we set the link distance of the desired user $r_D = 100$ m, and the threshold distance of the

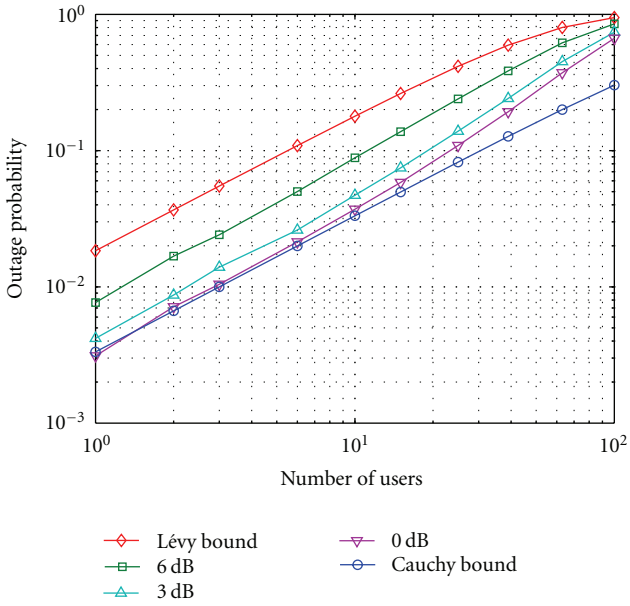

FIGURE 3: The outage probability P_{out} versus the number of users N_u in AWGN channels when $\alpha = 2$, $N_s = 10$, the shadowing standard derivations are, respectively, 0, 3, and 6 dB.

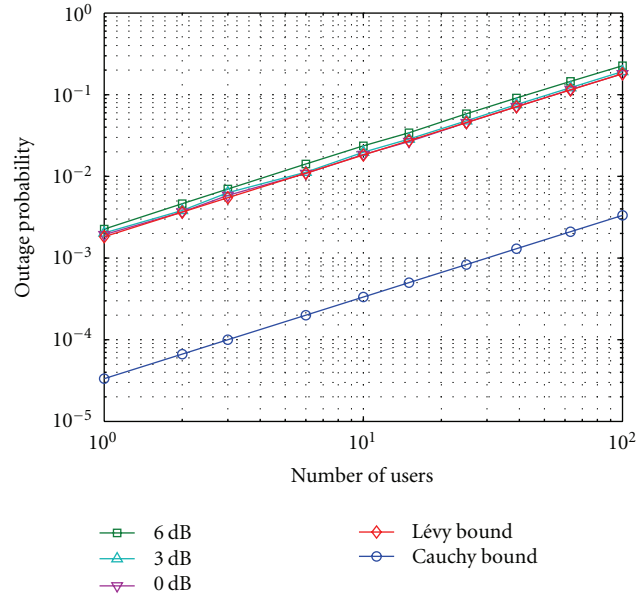

FIGURE 4: The outage probability P_{out} versus the number of users N_u in AWGN channels when $\alpha = 4$, $N_s = 10$, the shadowing standard derivations are, respectively, 0, 3, and 6 dB.

interference users $r_T = 1000$ m. Consider that the SNR of the desired user is 10 dB, and the required SINR is 4 dB, then the normalized interference power tolerance $\lambda_I = 0.3\lambda_D$.

The statistics of the interference power derived previously does not consider the shadowing. Shadowing is often modeled as a log-normal distribution, with its impact the PDF of interference power has no explicit expression any longer, but it is more close to Lévy distribution as will be shown in the simulations.

6.1. Outage Probability with $\alpha = 2$. We first verify the outage probability obtained in AWGN channel. The number of time slots in each frame is set to be $N_s = 10$. The outage probabilities obtained through numerical analysis and simulations are shown in Figure 3. The results of Cauchy bound and Lévy bound are obtained from (26). The curves labeled "0 dB", "3 dB", and "6 dB" are simulation results with corresponding standard derivations of shadowing. We can see that Cauchy bound is quite tight as a lower bound when the user number is less than 10 and the shadowing is low. When more users coexist in the network, the lower bound becomes loose. As we have mentioned, Lévy bound is an upper bound. With the increase of the shadowing standard derivation, the outage probability will gradually approach the upper bound.

6.2. Outage Probability with $\alpha = 4$. The numerical and simulated outage probabilities in this case of AWGN channel are presented in Figure 4. We can see that Cauchy bound is loose now, but Lévy bound is quite tight. Although with the increase of the shadowing standard derivation the simulated outage probabilities will exceed the upper bound, the differences between them are very small. The results shown in Figures 3 and 4 are consistent with our analysis in Section 3. Since the CDF of the standard Cauchy distribution is used for that of the single-sided Cauchy distribution with constraint $\lambda \geq 1$, the lower bound has some bias when users number is large.

6.3. Outage Probability with Interference Avoidance. When the desired user applies the interference avoidance technique, the numerical and simulation results in AWGN channels are shown in Figure 5, where $N_s = 4$ and shadowing is not considered. Here, Cauchy bound and Lévy bound are, respectively, obtained with $\alpha = 2$ and $\alpha = 4$, and the simulations are obtained with these two path loss factors as well. Comparing with the results in Figures 3 and 4, interference avoidance dramatically reduces the outage probabilities as expected, despite that using a smaller N_s increases the collision probability. Due to the power of N_s in the expression of the outage probability shown in (27), the bias of the Cauchy bound is amplified. Moreover, in this scenario, the Lévy bound is lower than the Cauchy bound. As can be seen from (23) and (26), this is because different interference tolerance λ_I is used in calculating the outage probability when different values of α are used.

6.4. Outage Probability in Multipath Channels. IEEE 802.15.4a channel model is used to generate the multipath channel response [33], where "CM3" environment is considered and the multipath delay spread $\tau_{\text{RMS}} = 10$ ns. In multipath channels, both the power and the duration of the interference signals are random variables in different channel realizations. The numerical results are obtained from (35), where the rectangle approximation of the average interference power profile is used. Figure 6 shows

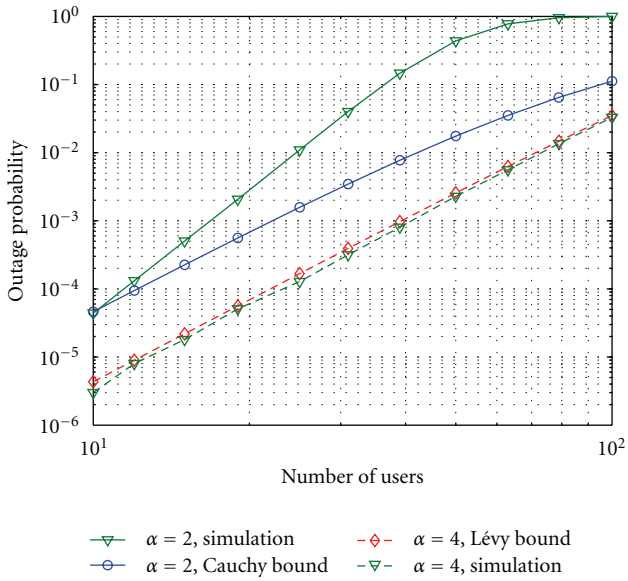

FIGURE 5: The outage probability P_{out} versus the number of users N_u in AWGN channels with interference avoidance, where $\alpha = 2$ for Cauchy bound and $\alpha = 4$ for Lévy bound, $N_s = 4$.

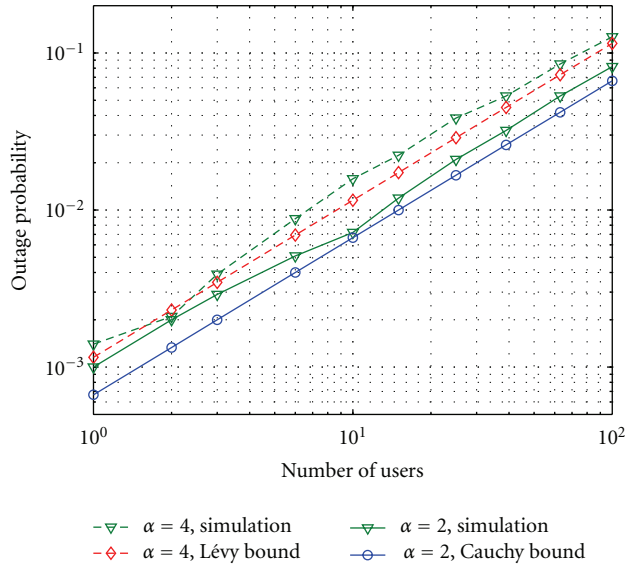

FIGURE 6: The outage probability P_{out} versus the number of users N_u in multipath channels, where $T_s = 100$ ns, $\tau_{\text{RMS}} = 10$ ns, $\alpha = 2$ and 4 are, respectively, simulated.

both the numerical and simulation results, where the pulse width $T_p = 1$ ns, the frame length $T_s = 100$ ns, and other conditions are the same with those in AWGN channels. Again, $\alpha = 2$ and $\alpha = 4$ are used, respectively, for Cauchy bound and Lévy bound, and the shadowing is not considered. The numerical results are shown to agree well with the simulation results. In this scenario, Lévy bound is higher than Cauchy bound. In addition to the influence of different λ_I, delay spread has different impact on these two bounds. As indicated by (43), longer delay spread will lead to higher Lévy bound, whereas Cauchy bound is independent of the delay spread.

7. Conclusion

In this paper, the spatial capacity of the IR-UWB networks with space-time focusing transmission is analyzed. We derived the upper and lower bounds of the outage probability for different path loss factors and then developed the closed-form expressions of the accommodable user density and the spatial capacity.

Analysis results showed that the spatial capacity is independent of the frame length and is associated with specific interference tolerance. The spatial capacity reduces with large path loss factor. Depending on the path loss factor being 2 or 4, the spatial capacity grows either linearly or sublinearly with the antenna number. Using more transmit antennas or shorter pulse is more efficient when the path loss factor is small. When the coverage of the UWB single-hop link extends, the accommodable user density should be reduced to guarantee a given outage probability, and thus the spatial capacity is also reduced. With TR prefiltering, long channel delay spread provides large spreading gain but also induces high collision probability among users. As a result, the spatial capacity will not increase with longer channel delay spread. Moreover, this leads to lower efficiency of using the bandwith and antenna resources when the path loss factor is large. To further improve the spatial capacity, we can employ advanced prefilters instead of the TR prefilter and apply the interference avoidance or interference alignment schemes.

Acknowledgment

This work was supported by the National Natural Science Foundation of China (NSFC) under Grant no. 60802015.

References

[1] J. Keignart, C. Abou-Rjeily, C. Delaveaud, and N. Daniele, "UWB SIMO channel measurements and simulations," *IEEE Transactions on Microwave Theory and Techniques*, vol. 54, no. 4, pp. 1812–1819, 2006.

[2] C. Zhou, N. Guo, and R. C. Qiu, "Time-reversed ultra-wideband (UWB) multiple input multiple output (MIMO) based on measured spatial channels," *IEEE Transactionson Vehicular Technology*, vol. 58, no. 6, pp. 2884–2898, 2009.

[3] M. Emami, M. Vu, J. Hansen, A. J. Paulraj, and G. Papanicolaou, "Matched filtering with rate back-off for low complexity communications in very large delay spread channels," in *Proceedings of the 38th Asilomar Conference on Signals, Systems and Computers (ACSSC '04)*, pp. 218–222, November 2004.

[4] T. Strohmer, M. Emami, J. Hansen, G. Papanicolaou, and A. J. Paulraj, "Application of time-reversal with MMSE equalizer to UWB communications," in *Proceedings of the IEEE Global Telecommunications Conference (GLOBECOM '04)*, pp. 3123–3127, December 2004.

[5] N. Guo, B. M. Sadler, and R. C. Qiu, "Reduced-complexity UWB time-reversal techniques and experimental results," *IEEE Transactions on Wireless Communications*, vol. 6, no. 12, pp. 4221–4226, 2007.

[6] A. Derode, P. Roux, and M. Fink, "Robust acoustic time reversal with high-order multiple scattering," *Physical Review Letters*, vol. 75, no. 23, pp. 4206–4209, 1995.

[7] D. Rouseff, D. R. Jackson, W. L. J. Fox, C. D. Jones, J. A. Ritcey, and D. R. Dowling, "Underwater acoustic communication by passive-phase conjugation: theory and experimental results," *IEEE Journal of Oceanic Engineering*, vol. 26, no. 4, pp. 821–831, 2001.

[8] J. L. Schwartz and B. D. Steinberg, "Ultrasparse, ultrawideband arrays," *IEEE Transactions on Ultrasonics, Ferroelectrics, and Frequency Control*, vol. 45, no. 2, pp. 376–393, 1998.

[9] M. G. M. Hussain, "Principles of space-time array processing for ultrawide-band impulse radar and radio communications," *IEEE Transactions on Vehicular Technology*, vol. 51, no. 3, pp. 393–403, 2002.

[10] F. Dowla and A. Spiridon, "Spotforming with an array of ultra-wideband radio transmitters," in *Proceedings of the IEEE Conference on Ultra Wideband Systems and Technologies (UWBST '03)*, pp. 172–175, 2003.

[11] H. T. Nguyen, I. Z. Kovcs, and P. C. F. Eggers, "A time reversal transmission approach for multiuser UWB communications," *IEEE Transactions on Antennas and Propagation*, vol. 54, pp. 3216–3224, 2006.

[12] H. T. Nguyen, J. B. Andersen, and G. F. Pedersen, "The potential use of time reversal techniques in multiple element antenna systems," *IEEE Communications Letters*, vol. 9, no. 1, pp. 40–42, 2005.

[13] H. T. Nguyen, J. B. Andersen, G. F. Pedersen, P. Kyritsi, and P. C. F. Eggers, "Time reversal in wireless communications: a measurement-based investigation," *IEEE Transactions on Wireless Communications*, vol. 5, no. 8, pp. 2242–2252, 2006.

[14] R. C. Qiu, C. Zhou, N. Guo, and J. Q. Zhang, "Time reversal with MISO for ultrawideband communications: experimental results," *IEEE Antennas and Wireless Propagation Letters*, vol. 5, no. 1, pp. 269–273, 2006.

[15] H. Nguyen, F. Zheng, and T. Kaiser, "Antenna selection for time reversal MIMO UWB systems," in *Proceedings of the IEEE 69th Vehicular Technology Conference (VTC '09)*, pp. 1–5, April 2009.

[16] X. Liu, B. Z. Wang, S. Xiao, and S. Lai, "Post-time-reversed MIMO ultrawideband transmission scheme," *IEEE Transactions on Antennas and Propagation*, vol. 58, no. 5, Article ID 5422614, pp. 1731–1738, 2010.

[17] H. El-Sallabi, P. Kyritsi, A. Paulraj, and G. Papanicolaou, "Experimental investigation on time reversal precoding for space-time focusing in wireless communications," *IEEE Transactions on Instrumentation and Measurement*, vol. 59, no. 6, pp. 1537–1543, 2010.

[18] Z. Liu, Y. Tian, and C. Yang, "A preprocessing algorithm of Ultra-wideband signal for space-time focusing transmission," in *Proceedings of the 9th International Conference on Signal Processing (ICSP '08)*, pp. 1896–1899, October 2008.

[19] H. Nguyen, Z. Zhao, F. Zheng, and T. Kaiser, "On the MSI mitigation for MIMO UWB time reversal systems," in *Proceedings of the IEEE International Conference on Ultra-Wideband (ICUWB '09)*, pp. 295–299, September 2009.

[20] YU. H. Chang, S. H. Tsai, X. Yu, and C. C. J. Kuo, "Ultrawideband transceiver design using channel phase precoding," *IEEE Transactions on Signal Processing*, vol. 55, no. 7, pp. 3807–3822, 2007.

[21] YU. H. Chang, S. H. Tsai, X. Yu, and C. C. J. Kuo, "Codeword design for ultra-wideband (UWB) precoding," *IEEE Transactions on Wireless Communications*, vol. 9, no. 1, pp. 198–207, 2010.

[22] P. Gupta and P. R. Kumar, "The capacity of wireless networks," *IEEE Transactions on Information Theory*, vol. 46, no. 2, pp. 388–404, 2000.

[23] S. P. Weber, X. Yang, J. G. Andrews, and G. de Veciana, "Transmission capacity of wireless ad hoc networks with outage constraints," *IEEE Transactions on Information Theory*, vol. 51, no. 12, pp. 4091–4102, 2005.

[24] C. Comaniciu and H. V. Poor, "On the capacity of mobile ad hoc networks with delay constraints," *IEEE Transactions on Wireless Communications*, vol. 5, no. 8, pp. 2061–2071, 2006.

[25] A. Goldsmith, *Wireless Communications*, Cambridge University Press, New York, NY, USA, 2005.

[26] J. P. Nolan, *Stable Distributions—Models for Heavy Tailed Data*, Birkhäuser, Boston, Mass, USA, 2010.

[27] V. R. Cadambe and S. A. Jafar, "Degrees of freedom of wireless networks—what a difference delay makes," in *Proceedings of the 41st Asilomar Conference on Signals, Systems and Computers (ACSSC '07)*, pp. 133–137, November 2007.

[28] V. R. Cadambe, S. A. Jafar, and S. Shamai, "Interference alignment on the deterministic channel and application to fully connected Gaussian interference networks," *IEEE Transactions on Information Theory*, vol. 55, no. 1, pp. 269–274, 2009.

[29] M. Z. Win and R. A. Scholtz, "Characterization of ultra-wide bandwidth wireless indoor channels: a communication-theoretic view," *IEEE Journal on Selected Areas in Communications*, vol. 20, no. 9, pp. 1613–1627, 2002.

[30] J. G. Proakis, *Digital Communications*, McGraw-Hill, New York, NY, USA, 4th edition, 2001.

[31] V. R. Cadambe and S. A. Jafar, "Interference alignment and degrees of freedom of the K-user interference channel," *IEEE Transactions on Information Theory*, vol. 54, no. 8, pp. 3425–3441, 2008.

[32] K. Gomadam, V. R. Cadambe, and S. A. Jafar, "Approaching the capacity of wireless networks through distributed interference alignment," in *Proceedings of the IEEE Global Telecommunications Conference (GlobeCom '08)*, pp. 1–6, 2008.

[33] A. F. Molisch, "Ultrawideband propagation channels-theory, measurement, and modeling," *IEEE Transactions on Vehicular Technology*, vol. 54, no. 5, pp. 1528–1545, 2005.